J. P. Gordon, Bell System Tech. J. 40, 489 (1961); G. D. Boyd and H. Kogelnik, *ibid.* 41, 347 (1962).

[8]R. P. Feynman, F. L. Vernon, Jr., and R. W. Hellworth, J. Appl. Phys. 28, 49 (1957).

[9]S. L. McCall and E. L. Hahn, in *The Physics of Quantum Electronics*, edited by S. F. Jacobs and J. B. Mandelbaum (Optical Sciences Center, The University of Arizona, Tucson, Ariz. 1968), pp. 65–99; C. K. Rhodes, A. Szoke, and A. Javan, Phys. Rev. Letters 16, 1151 (1968).

[10]F. V. Condon and G. H. Shortly, *The Theory of Atomic Spectra* (Cambridge U. P., London, 1957), p. 387.

[11]A. Frova, M. A. Duguay, C. G. B. Garrett, and S. L. McCall, J. Appl. Phys. 40, 3969 (1969).

[12]A. G. Fox, S. E. Schwarz, and P. W. Smith, Appl. Phys. Letters 12, 371 (1968).

[13]A. G. Fox and P. W. Smith, Phys. Rev. Letters 18, 826 (1967).

[14]M. A. Duguay and J. W. Hansen, IEEE J. Quantum Electron. QE-5, 326 (1969).

[15]C. K. N. Patel and R. E. Slusher, Phys. Rev. Letters 19, 1019 (1967).

PHYSICAL REVIEW A VOLUME 2, NUMBER 3 SEPTEMBER 1970

Nuclear Magnetic Resonance in Solid Helium-3–Helium-4 Mixtures between 0.3 and 2.0 °K *

D. S. Miyoshi, † R. M. Cotts, A. S. Greenberg, and R. C. Richardson
Laboratory of Atomic and Solid State Physics, Cornell University, Ithaca, New York 14850

(Received 29 August 1969)

Nuclear-magnetic-resonance techniques have been used to study vacancy diffusion and the exchange interaction of He^3 in solid He^3-He^4 mixtures between 0.3 and 2.0 °K for molar volumes between 20 and 22 cc/mole. The concentrations studies are 32.1, 7.78, and 1.94% He^3 in He^4. There is good agreement between the diffusion activation energies determined from the T_2 measurements and those obtained by measuring the diffusion constant directly using the field-gradient technique. These activation energies are consistently lower for mixtures than for pure He^3. The T_1 data in the Zeeman-exchange plateau region indicate that the exchange interaction is independent of concentration. The T_2 data in the exchange-narrowed region are not in agreement with the theoretical result obtained by allowing the moments of the line shape to become concentration dependent. The experimental values of T_2 are much lower than the predicted values. This deviation is qualitatively explained by postulating the existence of two spin species: those that strongly experience the effects of exchange and those that do not. A small fraction of the isolated spins can then dominate the T_2 relaxation process.

I. INTRODUCTION

The magnetic properties of solid He^3 have been the subject of intense experimental and theoretical investigation for the past ten years.[1–7] The most interesting feature of this solid is that the van der Waals binding energy is not much larger than the kinetic zero-point energy, so that the atoms undergo large-amplitude zero-point vibrations, and there is an unusually large amount of overlap between the wave functions of atoms occupying adjacent lattice sites. As a result of the atomic overlap and the symmetry requirements for pairs of fermions, there is a probability that a pair of atoms will mutually tunnel between adjacent lattice sites and interchange their positions. This process leads to an exchange energy in the Hamiltonian specifying the system.[8] The magnitude of the exchange interaction is essentially proportional to the electrostatic energy developed by the overlapping atoms and the scalar product of the nuclear-spin orientations. The exchange process appears to be most probable when the pair of atoms are in the singlet state.[6,7]

The effects of He^4 impurities in the He^3 lattice have also received experimental[9–14] and theoretical[15] attention. Recent nuclear resonance experiments seem to indicate that the excess volume around a He^4 impurity permits the neighboring pairs of He^3 atoms to have a greatly "enhanced" exchange interaction.[13,14] In this work, we have investigated the possibility of such effects from a different point of view. By studying the nuclear resonance properties of solid mixtures of He^3 and He^4 with He^3 concentrations between 2 and 30%, we hoped to understand what effects the He^4 would produce on neighboring He^3 atoms undergoing the exchange tunneling, and what effects the dilution process has on the spectral density function responsible for the relaxation processes.

In Sec. II, the theory of how diffusion and exchange affect T_1 and T_2 is reviewed and extended

to include the concentration dependence. Section III contains the experimental technique used to measure T_1 and T_2. The results and discussion are contained in Sec. IV, and the conclusions can be found in Sec. V.

II. THEORY

The theory of the line-shape and spin-lattice relaxation in pure solid He^3 has been discussed in detail elsewhere[2,5,16] and will only be summarized here in order to make a simple extension to the case of diluted He^3 spins in the He^4 lattice. In that which follows, the notation is essentially the same as that used, for instance, by Richardson, Landesman, Hunt, and Meyer[5] (RLHM). The exchange parameter J is defined with the dimensions of frequency such that the interaction Hamiltonian between a pair of spins i and j is $\mathcal{H}_{ex\,ij} = JI_i \cdot I_j$.

In pure He^3 solid, there are at least five distinct temperature regions in which different relaxation mechanisms govern the recovery of the nuclear magnetism to thermal equilibrium.[17] Here, we will be interested in the processes involved in the two highest-temperature regions called the classical diffusion region and the exchange "plateau" region. At these temperatures, above 0.3 °K for the samples we have studied, the exchange-energy reservoir is kept in good thermal equilibrium with the lattice by the diffusion of the atoms through the solid.[2] We may therefore characterize the thermal relaxation time of the magnetization by a single parameter T_1.

A. T_1 and T_2 in Diffusion Region

At the highest temperatures for which He^3 is a stable solid, the thermal and transverse relaxation times T_1 and T_2 are dominated by thermally activated diffusion. Reich[1] successfully used the treatment of diffusion by Bloembergen, Purcell, and Pound[18] (BPP) to describe the high-temperature relaxation processes in pure He^3. The Zeeman states of the spin system are connected to the lattice by fluctuations of the dipole field caused by the diffusion of the atoms through the lattice. The spatial variables in the dipolar Hamiltonian fluctuate randomly with time. BPP describe the fluctuations in the dipole field with a correlation function $g(\tau)$ proportional to $e^{-|\tau|/\tau_c}$, where the correlation time τ_c represents the average time spent by a spin in a particular site. For a liquid or powder of crystallites, the spin-lattice relaxation rate is given by

$$1/T_1 = J_1(\omega_0) + 4J_1(2\omega_0) , \tag{1}$$

where the spectral density function $J_1(\omega_0)$ is the Fourier transform of $g(\tau)$ and is given by

$$J_1(\omega_0) = \tfrac{2}{3} M_2 \tau_c / (1 + \omega_0^2 \tau_c^2) . \tag{2}$$

M_2 is the Van Vleck rigid-lattice second moment.[19] T_1 goes through a minimum at

$$\omega_0 \tau_c = 0.62 , \tag{3}$$

where

$$(T_1)_{\min} = 1.05\, \omega_0 / M_2 . \tag{4}$$

BPP further show that the spin-spin relaxation time T_2 depends on the spectral density functions in the following way:

$$1/T_2 = \tfrac{1}{4} J_0(0) = \tfrac{5}{2} J_1(\omega_0) + J_1(2\omega_0) . \tag{5}$$

The term $J_0(0)$ is due to the part of the dipolar Hamiltonian corresponding to the Zeeman transition $\Delta m = 0$, and is called the adiabatic part of T_2. The terms of $J_1(\omega_0)$ and $J_1(2\omega_0)$ are lifetime broadening terms and from the nonadiabatic part of T_2. Evaluation of the spectral density functions leads to the following result for T_2:

$$1/T_2 = \tfrac{2}{3} M_2 \left(\tfrac{3}{2} \tau_c + \tfrac{5}{2} \frac{\tau_c}{1 + \omega_0^2 \tau_c^2} + \frac{\tau_c}{1 + 4\omega_0^2 \tau_c^2} \right) . \tag{6}$$

Note that for $\omega_0 \tau \ll 1$, we have $1/T_2 = \frac{10}{3} M_2 \tau_c$, while for $\omega_0 \tau_c \ll 1$, we have $T_2^{-1} = M_2 \tau_c$. Since atomic diffusion is a thermally activated process, we have

$$\tau_c = \tau_0 e^{W/kT} , \tag{7}$$

where W is the activation energy and τ_0 is the correlation time at $1/T = 0$. If the measured values of T_2 are plotted against the reciprocal temperature on a semilogarithmic scale, a "step" will appear near the T_1 minimum owing to the "$\frac{10}{3}$ effect." In order to eliminate this step we can separate T_2 into its adiabatic and lifetime broadened terms

$$1/T_2 = 1/T_2' + R/T_1 , \tag{8}$$

where R varies from 0.70 to 1.38, depending on the value of $\omega_0 \tau_c$. The semilog plot of $1/T_2'$ versus $1/T$ should now show an exponential dependence, since we have

$$1/T_2' = M_2 \tau_c . \tag{9}$$

In order to express the concentration dependence of T_1 and T_2 in the diffusion region, the expression for M_2 must be investigated. In the case of a mixture, the Van Vleck second moment becomes (for spin $I = \frac{1}{2}$)

$$M_2 = \tfrac{9}{20} \gamma^4 h^2 \sum_{k=k'} r_{jk}^{-6} , \tag{10}$$

where k' refers to a site occupied by a He^3 atom. If all sites have an equal probability of being occupied, then the restricted sum can be replaced by x times the sum over all sites:

$$M_2(x) = x M_2(1) , \tag{11}$$

where x is the concentration of He^3 atoms. The T_1 minimum then becomes

$$(T_1)_{\min} = 1.05\,\omega_0/xM_2(1)\,, \tag{12}$$

and the adiabatic part of T_2 becomes

$$1/T_2' = xM_2(1)\,\tau_c\,. \tag{13}$$

B. T_1 and T_2 in Exchange "Plateau" Region

The effects of exchange on T_1 and T_2 in pure He^3 at temperatures above about 0.5 °K have been studied in detail.[1-5] The exchange interaction produces a motion between neighboring antiparallel spins, which is like a rotation of the two atoms about their center with an angular frequency ω_e, of order J. As a result of the exchange rotation or spin flipping, the spin variables of the dipolar Hamiltonian become time dependent. Anderson and Weiss[20] demonstrated that the exchange modulation of the dipolar field causes the resonance line to become narrower than that expected for a "rigid lattice." The result is similar to that obtained for diffusive motion of the spins except that in this case the spin variables rather than the spatial variables fluctuate randomly with time. Hartmann[16] successfully analyzed the T_1 process for this case by introducing a Gaussian correlation function $\exp(-\frac{1}{2}\omega_e^2\tau^2)$ to describe the exchange modulation of the dipolar field. The composite spectral density function for the relaxation in the presence of both atomic diffusion and exchange modulation is thus the Fourier transform of a correlation function containing the product of the exchange and diffusive motion, i.e.,

$$g(\tau) \sim \exp(-\tfrac{1}{2}\omega_e^2\tau^2)\exp(-|\tau|/\tau_c)\,.$$

At sufficiently low temperatures, when $\tau_c \ll 1/\omega_e$, the diffusion effects can be neglected and a temperature-independent spectral density is obtained:

$$J_1(\omega_0) = [(2\pi)^{1/2}M_2/3\omega_e]\,e^{-\omega_0^2/2\omega_e^2}\,, \tag{14}$$

which leads to a temperature-independent plateau in T_1 given by

$$1/T_1 = [(2\pi)^{1/2}M_2/3\omega_e](e^{-\omega_0^2/2\omega_e^2} + 4e^{-2\omega_0^2/\omega_e^2}), \tag{15}$$

and a low-temperature limit for T_2 given by

$$1/T_2 = [(2\pi)^{1/2}M_2/3\omega_e](\tfrac{3}{2} + \tfrac{5}{2}e^{-\omega_0^2/2\omega_e^2} + e^{-2\omega_0^2/\omega_e^2}), \tag{16}$$

where

$$\omega_e^2 = M_4/M_2 \tag{17}$$

and M_4 is the Van Vleck rigid-lattice fourth moment.

Expression (17) for ω_e is obtained in the Gaussian approximation by identifying the first three terms of a Taylor expansion of the first-order perturbation calculation of the correlation function,[21] with the Taylor expansion of

$$\exp(-\tfrac{1}{2}\omega_e^2\tau^2)\,.$$

RHLM studied the density and frequency dependence of T_1 and T_2 in pure He^3 in the exchange plateau region and found that in large applied magnetic fields, for which $\omega_0 > \omega_e$, the dependence of T_1 and T_2 on ω_0 is less than that predicted by the Gaussian approximation. However, they found that there does exist a single spectral density function which describes T_1 and T_2 for all values of ω_0 and ω_e throughout the bcc phase. In the hcp phase, a similar result was obtained but with a spectral function for which the Gaussian correlation function was apparently a better approximation.

The concentration dependence of T_1 and T_2 arises in a straightforward way through the behavior of ω_e and M_2. The exchange frequency depends on M_4, which can be written (for spin $I = \frac{1}{2}$)[22]:

$$M_4 = \frac{\gamma 4\hbar^2}{16N}\sum_{j,k,l\neq}[2J_{jk}^2(b_{jk}-b_{kl})^2 + 2J_{jk}J_{kl}(b_{jl}-b_{jk})(b_{jl}-b_{kl})]\,, \tag{18}$$

where N is the number of He^3 atoms in the solid, b_{jk} are position coefficients, and $\sum_{j,k,l\neq}$ means that all three summation indices must be different. In addition, only terms of the order J^2 have been kept, i.e., J is assumed to be much larger than the dipolar interaction. An examination of this summation shows that the sum over J gives the number of He^3 atoms N, and the restricted sum over occupied sites k and l gives x^2 times the sum over all sites:

$$M_4(x) = x^2 M_4(1)\,. \tag{19}$$

The concentration dependence of the exchange frequency can now be written, using the earlier results for pure He^3,[2]

$$\omega_e = 2.39\,x^{1/2}J \quad \text{for the bcc phase}, \qquad \omega_e = 3.24\,x^{1/2}J \quad \text{for the hcp phase}\,, \tag{20}$$

T_1 and T_2 become

$$\frac{1}{T_1} = \frac{(1.89\times10^{11})(x)}{\omega_e V^2}\times(e^{-\omega_0^2/2\omega_e^2} + 4e^{-2\omega_0^2/\omega_e^2})\,, \tag{21}$$

$$\frac{1}{T_2} = \frac{(1.89\times10^{11})(x)}{\omega_e V^2}\times(\tfrac{3}{2} + \tfrac{5}{2}e^{-\omega_0^2/2\omega_e^2} + e^{-2\omega_0^2/\omega_e^2})\,, \tag{22}$$

where the constant 1.89×10^{11} is calculated to be valid to within 1% for both the bcc and hcp phases.

III. EXPERIMENTAL TECHNIQUES

The experimental techniques used in this research are all well known. A pumped liquid He^4 bath was used to attain temperatures down to 1.2 °K, and a pumped liquid He^3 bath inside an ex-

change gas can was used for temperature between 1.2 and 0.3 °K. The NMR sample was introduced through a capillary tube (0.010 in. i.d.) that was kept in thermal contact with the He^3 bath. A constriction was created in the capillary by forcing into it the largest diameter wire possible. This was done so that the sample solution would first freeze at this point, thereby fixing the molar volume of the sample. The sample chamber shown in Fig. 1 was made out of *Kel-F* (obtained from Almac Plastics), a nylonlike substance that is easily machinable. The NMR coil was wound on the outside of the sample chamber, which had dimensions $\frac{1}{4}$ in. o.d., $\frac{1}{16}$ in. i.d., and $\frac{1}{2}$ in. length. The pressure of the sample was measured by means of a strain gauge, which consisted of a capacitor formed by two concentric cylinders.[23] The arrangement of the sample chamber and strain gauge are shown in Fig. 1.

The nuclear relaxation times T_1 and T_2 were measured using a single-coil pulse spectrometer based on the techniques first developed by Hahn.[24] The pulse spectrometer used a relatively low-power transmitter and coherent rf detection.[25] It

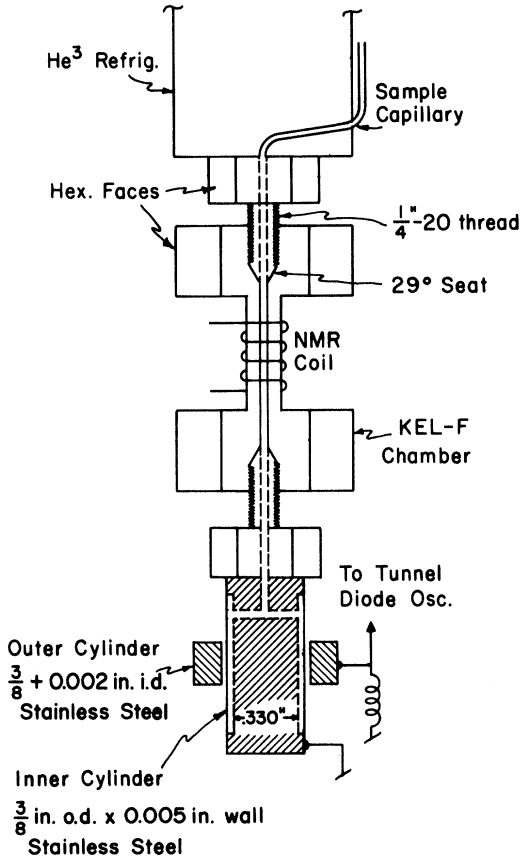

FIG. 1. Sample chamber and strain gauge.

was entirely transistorized, and could be operated from 0.2 to 20 MHz. A single-coil arrangement rather than crossed coils was chosen because the small coil volume meant that a low transmitter power was needed. The single coil consisted of a single layer of 50 turns of No. 40 wire, $\frac{1}{2}$ in. long, and $\frac{1}{4}$ in. diam. The natural resonant frequency of the coil in parallel with the capacity of the coaxial line was about 4 MHz. In order to operate below this frequency, a variable capacitor was placed in parallel with the coil. For frequencies higher than 4 MHz, a variable inductor was used to resonate the tuned circuit.

T_1 was determined by measuring the magnitude of the free induction decay following the second of a 90°-90° pulse sequence as a function of the time separation of the two pulses. T_2 was determined by one of two methods: If the linewidth was inhomogeneously broadened, then the spin-echo technique was used to determine T_2. In the high-pressure samples where the exchange interaction was small, T_2 was equal to the time at which the free induction decay decreased by a factor of $1/e$. The diffusion constant D was measured by applying a magnetic-field gradient G across the sample and studying the time dependence of the transverse magnetization.[26]

IV. RESULTS AND DISCUSSION

A. Determination of Melting Curve

Because of the strong dependence of the experimental parameters on the molar volume of the sample, a great deal of time and effort was spent in determining the molar volume to within 0.1 cm^3. This was done by carefully measuring the pressure in the sample, and then converting it to a molar volume by means of an equation given by Mullin[27]:

$$V(x, P) = xV_3(1, P) + (1-x)V_4(0, P) - Cx(1-x) , \quad (23)$$

where $V(x, P)$ is the molar volume of the He^3-He^4 mixture, x is the concentration of He^3, $V_3(1, P)$ and $V_4(0, P)$ are the molar volumes of pure He^3 and He^4, respectively,[28,29] and the constant C is a small correction factor given by

$$C = 0.4 \text{ cm}^3/\text{mole} . \quad (24)$$

This equation is plotted in Fig. 2 for He^3 concentrations $x = 0.321$, 0.0778, and 0.0194, as well as for pure He^3 and pure He^4. Note that Eq. (23) holds only for pressures above 29 atm, as pure He^3 is a liquid for lower pressures. Since the pressure of the He^3-He^4 solid was often less than 29 atm, the curves for the mixtures had to be extrapolated to lower pressures.

The discontinuity in volume associated with the bcc-hcp phase change has been neglected in Eq.

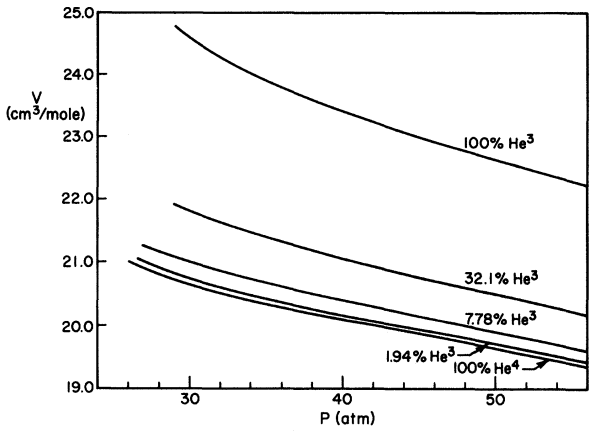

FIG. 2. Molar volume versus pressure for He^3-He^4 mixtures. (After Mullin, Ref. 27.)

(23) and in Fig. 2. For the purposes of volume calculation in this work, it is assumed that Eq. (23) represents the volume variation in going from pure bcc He^3 (with $x = 1.0$) to pure hcp He^4 (with $x = 0$). In pure He^3, the magnitude of the discontinuity is 0.1 cm^3,[8] therefore the error in volume determination using Eq. (23) is expected to be less than 0.1 cm^3.

Careful measurements of sample pressure as a function of temperature permitted us to determine the boundaries between the various solid phases and the boundary between the liquid phase and the solid phase, the melting curve. Figure 3 shows the melting curve for a 32% He^3 sample, as well as the boundaries for the bcc, hcp, and the bcc-hcp mixed phases. Solid samples were prepared by cooling the liquid under constant pressure from an initial point below the melting curve. When the sample temperature intersected the melting curve a solid block formed in the capillary fill line and the sample pressure then decreased rapidly with decreasing temperature, thus tracing the melting curve. At sufficiently low temperatures, the sample chamber became completely filled with solid and the sample pressure became less sensitive to changes in temperatures. There did exist a mild temperature dependence in the solid due to thermal contraction, but this vanished at temperatures a few tenths of a degree lower than the melting curve. Whenever a phase boundary was crossed (bcc mixed, mixed hcp), the thermal contraction gave rise to a cusp in the P-versus-T plot. The phase boundaries located by these pressure slope changes are called "pressure data" on the figure.

The NMR relaxation times T_1 and T_2 could also be used to determine the phase of the solid at a given temperature. Since the activation energies in the hcp phase were generally larger than those in the bcc phase, the diffusion regions were characterized by T_1's and T_2's which were strongly temperature dependent for the hcp phase, and much more weakly so for the bcc phase. In the exchange region, the hcp phase was characterized by a longer T_1 and a shorter T_2 than the bcc phase. However, these differences, though real, became apparent only after several data runs were made. The striking difference between the relaxation behavior in the two phases was readily distinguishable in mixed phase samples in which T_1 and T_2 were obviously the sum of two exponentials. In fact, if the sample were cooled while in the mixed phase region, the relative intensities of the two exponentials would often change, indicating that the number ratio of "bcc spins" to "hcp spins" was also changing. The results of this analysis are shown in the figure as open, closed and half-closed circles, representing the bcc, hcp, and mixed phases, respectively. Where the data have not been sufficient to firmly establish the phase boundaries, dashed lines have been used. Figures 4 and 5 show similar graphs for 7.78 and 1.94% He^3.

B. T_1 in Diffusion Region

Of the 14 different samples tested in this experiment, only eight showed a minimum in T_1 at a Larmor frequency of 3.50 MHz. In the other samples, the T_1 minimum was either obscured by the melting of the solid or overwhelmed by the effects of exchange. In these two cases, no minimum was

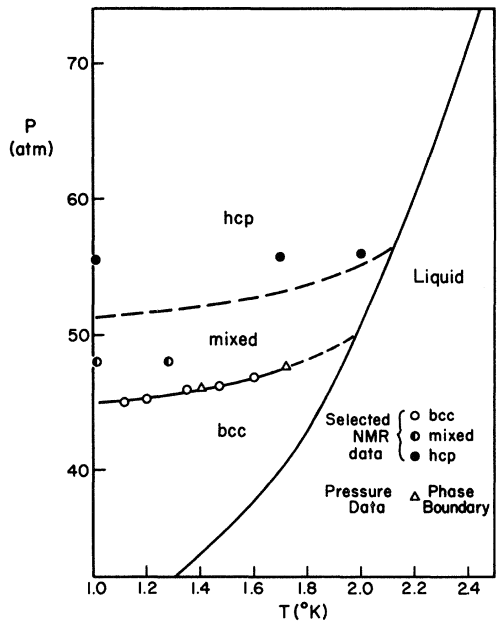

FIG. 3. Phase diagram in the P-T plane for 32.1% He^3.

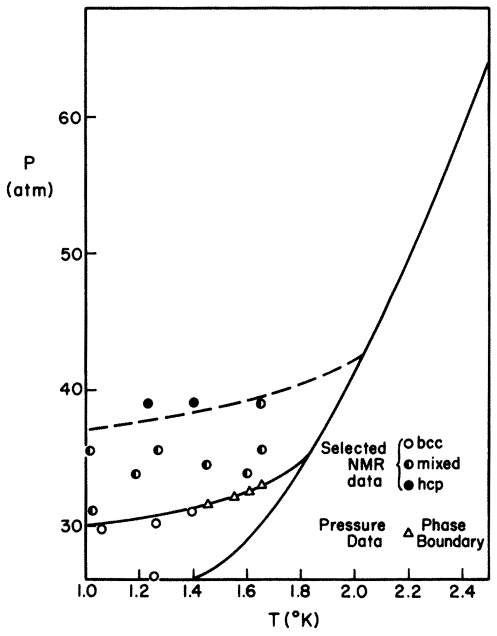

FIG. 4. Phase diagram in the P-T plane for 7.78% He^3.

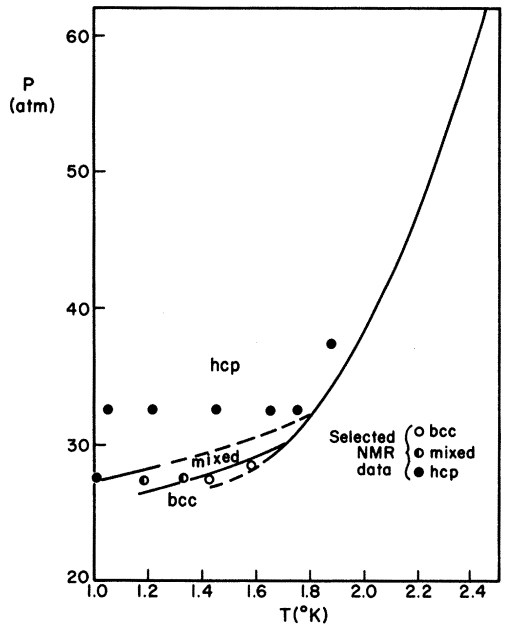

FIG. 5. Phase diagram in the P-T plane for 1.94% He^3.

observed. The values of the minimum in T_1 and the temperature at which it occurred are given in the first two data columns in Table I. The large errors in both quantities arise from scatter in the data and the large temperature intervals at which data was taken. Note also that most of the error in the T_1 minimum data is toward lower values. The unsymmetric error spread is due to the limited number of measurements in the vicinity of the minimum. As a result of the value of the T_1 minimum is more likely to be lower than the lowest experimental point than higher.

TABLE I. T_1 measurements in the duffusion region.

Concentration	V (cm^3/mole)	Phase	$(T_1)_{min}$ (sec)	$1/T$ at $(T_1)_{min}$ (°K^{-1})	W/k (°K)	Diffusion coefficient ($\times 10^{-8}$ cm^2/sec) Theoretical $D=a^2/6\tau_c$ at $(T_1)_{min}$ BPP	Torrey	Direct measurement using field gradient
32.1%	20.8	bcc	0.2 ± 0.05	0.8 ± 0.1	10 ± 1	1.6	0.9	1 ± 0.3
	20.2	hcp	$0.5^{+0.1}_{-0.2}$	0.5 ± 0.1	16 ± 2	1.7	1.0	...
7.78%	21.0	bcc	0.8 ± 0.4	0.9 ± 0.1	8.5 ± 0.5	4.1	2.4	1.5 ± 0.5
	20.6	bcc	1 ± 0.5	0.7 ± 0.1	10.5 ± 0	4.1	2.4	3 ± 1
	20.4	hcp	$2^{+0.5}_{-1.0}$	0.5 ± 0.1	...	4.0	2.5	...
1.94%	21.0	bcc	5 ± 2	0.7 ± 0.1	11 ± 1	10	6.1	4 ± 2
	20.6	hcp	6^{+2}_{-3}	0.6 ± 0.1	15 ± 2	11	6.4	5 ± 1
	20.3	hcp	3 ± 1	0.5 ± 0.1	20 ± 2	11	6.3	...

Figure 6 shows that values of the T_1 minimum plotted as a function of He^3 concentration, with representative experimental errors shown for each concentration. Also included in the figure is the datum point of Reich[1] for $x = 1.00$ that has been corrected for the difference in Larmor frequency (Reich used a frequency of 5.22 MHz). Equation (4) has been evaluated for the molar volumes 20.0 and 21.0 cm^3/mole and is represented by the two solid lines in the figure. The $(1/x)$ dependence of the data is demonstrated, although the deviation from the theory towards higher values of T_1 is evident. Much of the departure from theory can be attributed to the systematic error involved in determining T_1, as mentioned earlier. In addition, Hartmann[16] has shown that if the value of T_1 in the Zeeman-exchange region is near that of the T_1 minimum (within about a factor of 5), then exchange effects will reduce the effectiveness of the dipolar interaction, resulting in a T_1 minimum that is higher than that predicted by BPP or Torrey.

The T_1 data in the diffusion region were also analyzed to give an activation energy by the technique used by Holcomb and Norberg.[30] These activation energies are given in the third data column of Table I. In the case of the 1.94% bcc sample at 21 cm^3, the T_1 minimum occurred at the phase separation temperature, and the value of W/k is an upper limit obtained from analysis of a mixed-phase nonexponential recovery at the lower temperatures.

The diffusion constant at the temperature of the T_1 minimum was determined by the relation

$$D = a^2/6\tau_c, \tag{25}$$

where τ_c is given by Eq. (3) for the BPP theory. For the Torrey[31] theory, we have

$$\tau_c = 1.05/\omega_0 . \tag{26}$$

The values of D as determined by the BPP and Torrey theories are included in Table I along with the results of the direct measurement of the diffusion constant. The measured values of the diffusion constant appears to be in better agreement with the Torrey theory than the BPP theory.

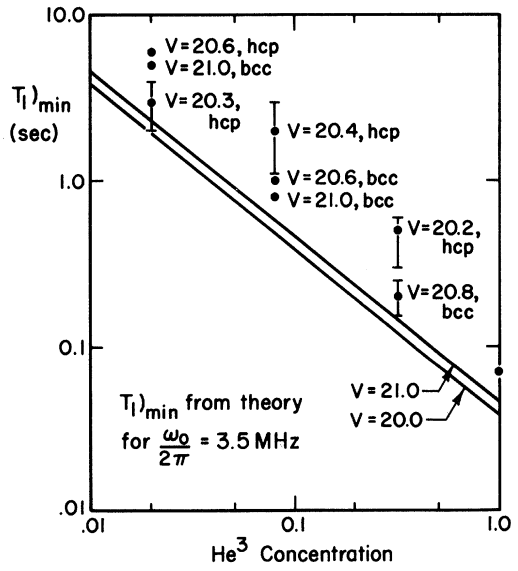

FIG. 6. T_1 minimum as a function of He^3 concentration for a larmor frequency of 3.50 MHz.

C. T_2 in Diffusion Region

T_2 in the high-temperature region had the exponential dependence on temperatures that is characteristic of thermally activated diffusion. Near the melting point of the solid in the bcc phase, the magnitudes of T_1 and T_2 were the same within the experimental error of T_1, although T_2 was smaller in almost all cases. In the hcp phase, the high-temperature side of the T_1 minimum could never be reached, so T_2 was always much less than T_1. The decay of the spin-echo envelope was always exponential (with the exception of the mixed-phase samples, where the sum of two exponentials was observed), which indicated that the line shapes were essentially Lorentzian.

The analysis of the T_2 data followed one of two methods, depending on whether or not a T_1 minimum existed. If a T_1 minimum did exist, the T_1 contribution to T_2 was subtracted using Eq. (8) yielding T_2'. The activation energy was then obtained from the slope of the semilog plot of T_2' versus $1/T$, by using a least-squares fit. The results of this method of analysis are given in Table II under the heading T_2'.

If a T_1 minimum did not exist, only the data near the melting point were used in the analysis, in the hope that R would be fairly constant in this region. The least-squares-fit program was again used to obtain activation energies, and these are listed under the heading T_2. The activation energies from the direct diffusion measurements (to be discussed below) are included in the column headed D, and the results from the preceding section on T_1 are listed under the heading T_1. There is generally good agreement between the results of all four methods. From these experimental values of W, an average activation energy for each sample has been determined. As in the case of 100% He^3, W decreases with increasing molar volume. At a given molar volume the activation energy is always less for a mixture than for pure He^3; and it is evident that the activation energy for the hcp phase is always higher than that of the bcc phase.

TABLE II. T_2 measurements in the diffusion region.

He^3 Concentration	V, phase (cm^3/mole)	Activation energy W From T_2 (°K)	From T_2' (°K)	From D (°K)	From T_1 (°K)	$\frac{W_{ave}}{k}$ (°K)	Melting point T_m (°K)	Direct diffusion data diffusion coefficient D at D_0 ($\times 10^{-5}$) cm^2/sec	D_{melt} ($\times 10^{-5}$) cm^2/sec	$(T_1)_{min}$ ($\times 10^{-8}$) cm^2/sec
31.1 %	21.7 bcc	5 ±0.5				5±0.5	1.3±0.1			
	21.4 bcc	6.5±0.5		5±1		6±0.5	1.45±0.1	0.2−1	14±2	
	21.0 bcc	10 ±1		8±1		9±1	1.8±0.1	1−3	12±2	
	20.8 bcc		9±1	11±1	10±1	10±1	1.9±0.1	2−6	18±3	1±0.3
	20.4 bcc	11 ±1		14±3		12±1	2.05±0.1	8−40	24±6	
	20.2 hcp				16±2	16±2	2.15±0.1			
7.78%	21.4 bcc	5 ±0.5		6±1		5.5±0.5	1.3±0.1	0.3−3	16±4	
	21.0 bcc		7.5±1	7.5±1	8.5±1	7.5±1	1.7±0.1	0.6−1.5	14±2	1.5±0.5
	20.6 bcc		9.5±0.5	9±1	10.5±1	9.5±1	1.85±0.1	1−4	18±1	3±1
	20.6 hcp	14 ±2				14±2	1.85±0.1			
	20.4 hcp	18 ±2				18±2	1.95±0.1			
1.94%	21.0 bcc		11±2		12±1	11±1	1.6±0.1	5−15	14±2	4±2
	21.0 hcp	15 ±1				15±1	1.6±0.1			
	20.6 hcp	18 ±2		14±4	15±2	16±2	1.8±0.1	2−15	8±1	5±1
	20.3 hcp	15 ±2			20±2	18±2	2.0±0.1			

The melting point of each sample has been noted under the heading T_m in Table II. The graph of W versus T_m for the bcc phase shown on Fig. 7 is a straight line for the 32 and 8% concentrations. The slope of the line $\Delta W/k\Delta T_m$ is about eight, and W/kT_m varies from four to six, which is much less than the value of 21 for the other rare gases.[32–34] Even in the hcp phase, W/kT_m is at most about nine for the samples studied.

The diffusion constant was measured directly using an applied field gradient[26] for nine of the samples tested. From these measurements at various temperatures, an activation energy was obtained, as well as the high-temperature intercept of D. The diffusion constant could thus be written

$$D = D_0 e^{-W/kT}, \tag{27}$$

where D_0 is the high-temperature intercept of D. From this equation, a value for D at the melting point D_{melt} was obtained as well as the value of D at the T_1 minimum.

Since the diffusion constant could only be measured for values greater than 10^{-8} cm^2/sec, the temperature range over which data could be taken was very small. Consequently, the activation energies obtained and particularly D_0 were subject to large errors as shown in Table II. The data for D_0 is presented as a range of values to emphasize the magnitude of the experimental error involved. For 100% He^3, Reich found that his results for D_0 were within a factor of 2 of the diffusion constant of the liquid $D_0 \approx 3\times 10^{-5}$ cm^2/sec. The results of the present experiment are within a factor of 4 of this value.

The diffusion constants at the melting point and the T_1 minimum are more accurately known because they were large enough to be measured. D_{melt} appears to be independent of concentration, phase, and molar volume, and agrees quite well with the range of values found by Reich for pure He^3.

D. T_1 in Zeeman-Exchange Plateau Region

The spin-lattice relaxation time T_1 was measured in the Zeeman-exchange plateau region for various combinations of molar volume, phase, and He^3 concentration. In each sample, the Larmor fre-

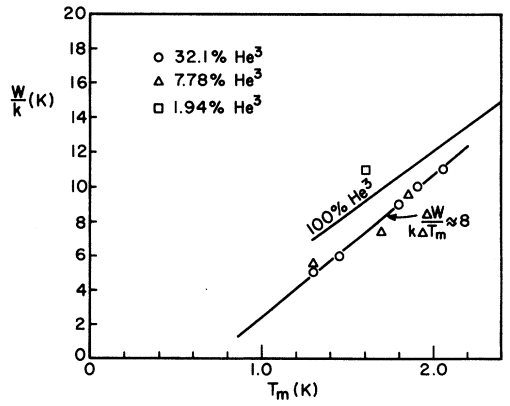

FIG. 7. Average activation energy as a function of the melting temperature for the bcc phase.

quency was varied over a wide range in order to investigate the frequency dependence of T_1 in the plateau region.

The measured values of T_1 expressed in sec are shown in Table III for the bcc and hcp phases. The error in determining T_1 at a given Larmor frequency and He^3 concentration was essentially independent of molar volume. The uncertainty has been expressed as a percentage and is lifted to the right of each group of data. The error increases with decreasing Larmor frequency and He^3 concentration because of the decreasing signal-to-noise ratio. The minimum error is about 10%.

Also shown in the table are values of the exchange interaction for 100% He^3 as obtained from the T_2 data of Richardson, Hunt, and Meyer,[4] of Garwin and Landesman,[2] and of Reich.[1] These values of J were derived from Fig. 8, which summarizes the results of these three research groups. Results of Garwin and Landesman for the hcp phase have been taken directly from their article, but the T_2 data of Richardson, Hunt, and Meyer, and the data of Reich were recalculated with the correct fourth moment[5] to yield values of J.

At low fields ($\omega_0 \ll \omega_e$), the expression for T_1 given in Eq. (21) becomes

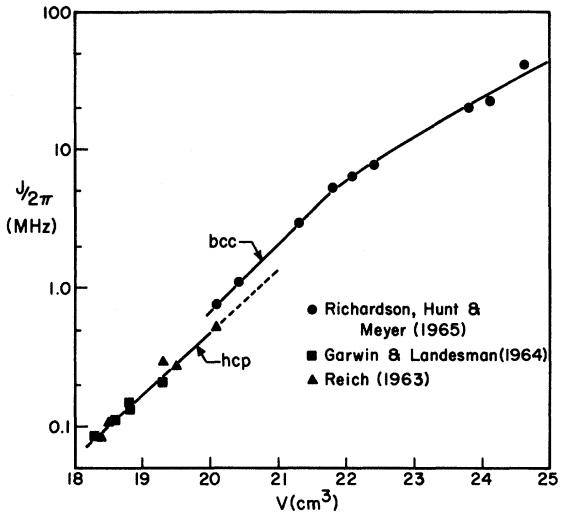

FIG. 8. Exchange interaction as a function of the molar volume for the bcc and hcp phases.

$$1/T_1(0) = 9.45\times10^{11}(x)/\omega_e V^2 , \qquad (28)$$

where $T_1(0)$ is the zero-field value of T_1. Table III contains the values of $T_1(0)$ calculated for each sample. ω_e is evaluated using Eq. (20) and the

TABLE III. T_1, J, and $T_1(0)$ in the Zeeman-exchange plateau region.

bcc phase

	$\omega_0/2\pi$	32.1% He^3 Molar volume				7.78% He^3 Molar volume			
	(MHz)	21.7 cm^3	21.4 cm^3	21.0 cm^3	Error	21.4 cm^3	21.0 cm^3	20.6 cm^3	Error
	0.70			0.033	25%				
Value of	1.00			0.039	20%	0.15		0.24	25%
	1.40	0.10	0.072	0.050	15%				
T_1	2.00	0.12	0.100	0.062	10%	0.45	0.90	1.2	15%
	3.50	0.17	0.19	0.175	10%	1.5	3.5	8.0	10%
(sec)	5.50	0.26	0.32	0.30	10%	5.5	16		10%
	6.74	0.35			10%	12.			10%
$J/2\pi$ (MHz)		4.8	3.3	2.0		3.3	2.0	1.3	
$T_1(0)$ (sec)		0.064	0.044	0.024		0.085	0.050	0.032	

hcp phase

	$\omega_0/2\pi$	32.1% He^3 Molar volume			7.78% He^3 Molar volume			1.94% He^3 Molar volume			
	(MHz)	20.6 cm^3	20.2 cm^3	Error	20.6 cm^3	20.4 cm^3	Error	21.0 cm^3	20.6 cm^3	20.3 cm^3	Error
Value of	0.57		0.022	35%							
	0.70		0.030	25%							
T_1	1.00	0.050	0.054	20%	0.45		25%	1.6	5.5		40%
	1.40	0.090	0.11	15%		1.3	20%	5.5	12	23	30%
(sec)	2.00	0.17	0.33	10%	2.2	4.0	15%	10	27	70	25%
	3.50	0.80	2.6	10%	12	25	10%	40	100	220	20%
$J/2\pi$ (MHz)		0.90	0.60		0.90	0.72		1.30	0.90	0.65	
$T_1(0)$ (sec)		0.015	0.0095		0.030	0.023		0.088	0.059	0.041	

values of J are assumed to be those of pure He^3 at the same molar volume. Figure 9 is a reduced plot of all the data for the bcc phase. The solid line is calculated from the spectral density function for bcc He^3 given by RLHM,

$$\frac{J_1(\omega_0)}{J_1(0)} = \tfrac{1}{5}\exp\left(\frac{-1.0(\omega_0/\omega_e)^2}{(\omega_0/\omega_e)+0.2}\right), \tag{29}$$

and is

$$\frac{T_1(0)}{T_1} = \tfrac{1}{5}\exp\left(\frac{-1.0(\omega_0/\omega_e)^2}{(\omega_0/\omega_e)+0.2}\right) + \tfrac{4}{5}\exp\left(\frac{-4.0(\omega_0/\omega_e)^2}{(2\omega_0/\omega_e)+0.2}\right). \tag{30}$$

The data for the mixtures also appear to agree very well with the 100% curve, which implies that the spectral density function given by Eq. (29) holds for these He^3 concentrations. The good fit is even more remarkable because the T_1 data is not arbitrarily normalized for a "best fit." $T_1(0)$ is a calculated quantity that depends only on J for a given molar volume and He^3 concentration. In this figure J has been chosen equal to its value for pure He^3 to demonstrate how little the exchange interaction depends upon concentration. If the value of J for each molar volume and concentration is varied to obtain a better fit of the points in Fig. 9 to the curve for pure He^3, the maximum change in J is less than 10%, which is the same order as the precision of the determination of J for pure He^3. The experiment may not be readily extended to lower concentration and larger molar volumes for the bcc phase because in the limit of practically pure He^4 the bcc phase exists only in a small region of pressure at high temperatures for which

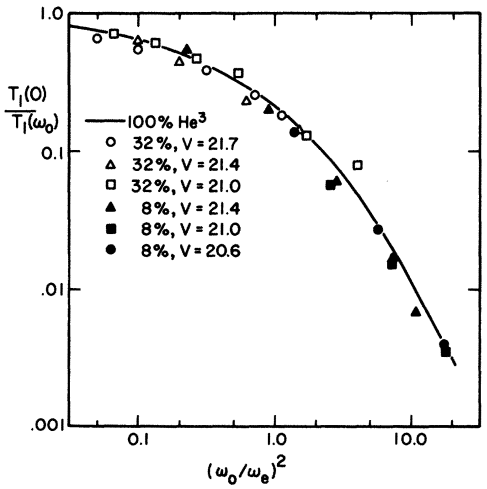

FIG. 9. $T_1(0)/T_1$ as a function of $\omega_0/\omega_e)^2$ for the bcc phase with $J(V)/2\pi$ assumed to be the value for pure He^3.

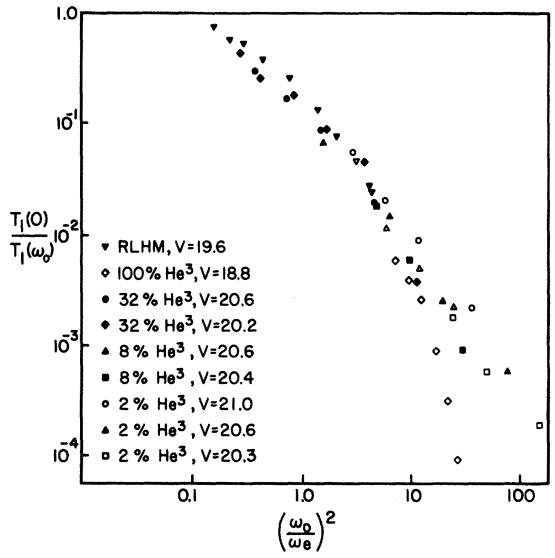

FIG. 10. $T_1(0)/T_1$ as a function of $\omega_0/\omega_e)^2$ for hcp phase with $J(V)/2\pi$ assumed to be the value for pure He^3.

the relaxation properties are always determined by atomic diffusion.

The hcp phase was also investigated. Figure 10 shows the results with J assumed to be equal to its value for pure He^3. The open diamonds are new measurements of $T_1(\omega_0)$ in the hcp phase for pure He^3 at a molar volume of 18.8 cm^3. The values are listed in Table IV. The data of RHLM in the hcp phase were found to be in agreement with the Gaussian correlation function over the range of ω_0/ω_e investigated. These new data for pure He^3 indicate that if one extends the measurements of T_1 to larger values of ω_0/ω_e than RLHM, the Gaussian approximation is not quite correct and that the spectral density can be better described by

$$\frac{J_1(\omega_0)}{J_1(0)} = \tfrac{1}{5}\exp\left(\frac{-1.6(\omega_0/\omega_e)^2}{(\omega_0/\omega_e)+1.0}\right). \tag{31}$$

As in the bcc phase, a single spectral density function will describe the field dependence of T_1 for values of $(\omega_0/\omega_e)^2$ less than 10. However, for larger ratios of $(\omega_0/\omega_e)^2$, the diluted mixtures relax somewhat faster than the pure He^3 would predict, indicating that there could be a slight concentration dependence to the spectral density function. If J is once again varied for each molar and concentration to obtain a more consistent fit to the rest of the data, the maximum change in J is of the order of 10%.

E. T_2 in Exchange-Narrowed Region

T_2 in the exchange-narrowed region showed the expected temperature independence. In some sam-

TABLE IV. T_1 measurements in plateau region at $V=18.8$ cm^3 in the hcp phase. The experimental error is less than 10%. The average value of T_2 for all fields was 3.8 msec. $T_1(0)=1.14$ msec, $\omega_e/2\pi = 0.49$ MHz.

$\omega_0/2\pi$ (MHz)	T_1 (sec)
1.30	0.20
1.50	0.30
1.70	0.44
2.00	1.3
2.25	3.7
2.50	12.5

ples T_2 was so short that the free-induction decay was greatly affected. In these cases the free-induction decay was used to determine T_2. Both the free-induction decay and the spin-echo decay were exponential, which indicated that the line shapes were Lorentzian.

The measured values of T_2, expressed in m sec, are shown in Table V for the bcc and hcp phases. The estimated error in T_2 is expressed as a percentage and is listed to the right of each group of data. These percentages are the same as for the T_1 table presented earlier.

These data were analyzed by comparing their frequency dependence to the frequency dependence of the ratio

$$\frac{T_2(0)}{T_2(\omega_0)} = \frac{3}{10} + \frac{1}{2}\frac{J_1(\omega_0)}{J_1(0)} + \frac{1}{5}\frac{J_1(\omega_0)}{J_1(0)} , \qquad (32)$$

where $T_2(0)$ is the zero-field value of T_2, and $J_1(\omega_0)/J_1(0)$ is given by Eq. (29) for the bcc phase and Eq. (31) for the hcp phase. The objective of this comparison was to obtain a value for $T_2(0)$ for each molar volume and He^3 concentration, which could then be checked with the theory. The exchange interaction was assumed equal to its value for pure He^3, since this assumption was successful in the analysis of the T_1 data.

The frequency dependence of the data was somewhat smaller than expected so there is a large uncertainty in the values of $T_2(0)$ obtained (at most 20% for the bcc phase, 30% for the hcp phase). These values of $T_2(0)$ are plotted as a function of He^3 concentration in Fig. 11. The dashed lines show the expected concentration dependence as given by the exchange theory with $\omega_0 = 0$:

$$1/T_2(0) = (5x)(1.89\times10^{11})/\omega_e V^2 , \qquad (33)$$

since $\omega_e \sim \sqrt{x}$, $T_2(0) \sim 1/\sqrt{x}$.

Also shown in the figure is the expected value of T_2 for $J=0$. The problem of the dilute spin system in a dipolar solid has been discussed in detail by Kittel and Abrahams.[35] They show that for $x>0.1$, the line has a Gaussian shape (with T_2 having a $1/\sqrt{x}$ concentration dependence), and that for $x<0.01$ the line has a Lorentzian shape (with T_2 having a $1/x$ concentration dependence).

The T_2 data is seen to fall between the exchange theory and the $J=0$ theory. This deviation from

TABLE V. T_2 in Zeeman-exchange plateau region.

	bcc phase T_2(msec)							
	32.1% He^3 Molar volume				7.78% He^3 Molar volume			
$\omega_0/2\pi$ (MHz)	21.7 cm^3	21.4 cm^3	21.0 cm^3	Error	21.4 cm^3	21.0 cm^3	20.6 cm^3	Error
0.70			27	25%				
1.00			34	20%	25			25%
1.40	60	32	31	15%		19		20%
2.00	65	37	34	10%	34	18		15%
3.50	75	38	41	10%	40	22	13	10%
5.50	78	46	43	10%	45			10%
6.74	90			10%				

	hcp phase T_2(msec)									
	32.1% He^3 Molar volume			7.78% He^3 Molar volume			1.94% He^3 Molar volume			
$\omega_0/2\pi$ (MHz)	20.6 cm^3	20.2 cm^3	Error	20.6 cm^3	20.4 cm^3	Error	21.0 cm^3	20.6 cm^3	20.3 cm^3	Error
0.57		3.5	35%							
0.70	7.5	4.0	25%							
1.00	8.8	4.2	20%	5.0		25%	8			40%
1.40	7.8	4.3	15%		1.8	20%	9	7	3.5	30%
2.00	8.5	5.4	10%	4.5	2.7	15%	10	7	2.5	25%
3.50	9.0	4.8	10%	4.5	2.4	10%	10	6.5	2.8	20%

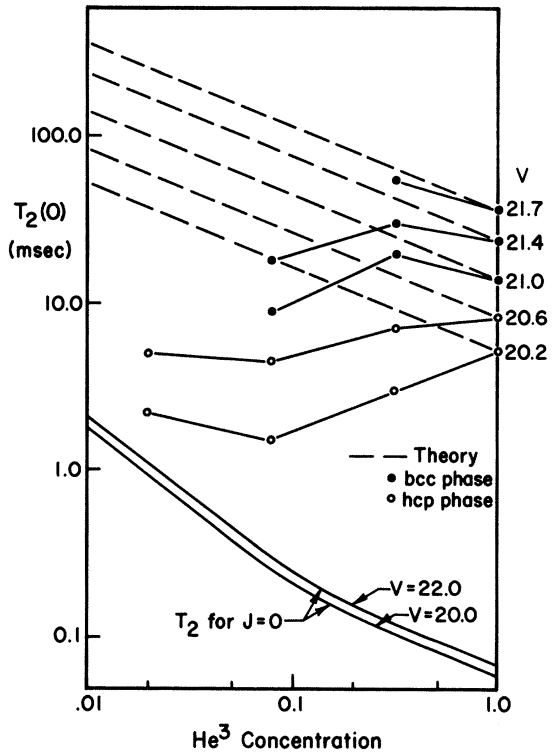

FIG. 11. Low-field value of T_2 as a function of He^3 concentration.

the exchange theory is well outside the experimental error and seems to be a real effect. This effect has also been observed in a few EPR experiments (see Glebashev[36] and Kumagai *et al.*[37]). It can be qualitatively explained by considering the statistics of the problem and the manner in which T_2 is determined. Suppose that there exist in the solid two types of spins: those that strongly experience the effects of exchange (type A) and those that do not (type B). Since all spins in the solid are coupled by the dipolar interaction, they must all relax with one characteristic time given by

$$1/T_2=(1-c)/T_{2A}+c/T_{2B}\,, \tag{34}$$

where T_{2A} and T_{2B} are the relaxation times of spins A and B, respectively, and c represents the fraction of all spins that are of type B. T_{2A} will fall on one of the dashed lines for a given He^3 concentration and molar volume, and T_{2B} will be of the order of $T_2(J=0)$. T_{2A} is therefore several orders of magnitude larger than T_{2B}. This means that c need only be a percent or so before the contribution of the B-type spin begins to dominate the relaxation rate. As the concentration of He^3 is reduced, more and more spins will become of type B, which accounts for the increasing deviation from the exchange theory.

This effect is not seen in the T_1 data because T_1 for exchange-affected spins (T_{1A}) is much less than T_1 for $J=0$ (T_{1B}). The equation

$$1/T_1=(1-c)/T_{1A}+c/T_{1B} \tag{35}$$

shows that c must be near unity in order to affect T_1. (See note added in proof.)

V. CONCLUSIONS

The primary objectives of this investigation were to study the behavior of diffusion and exchange in solid He^3-He^4 mixtures, and to extend previous theoretical calculations to include arbitrary He^3 concentrations, x.

The concentration dependence of the diffusion minimum in T_1 appears to follow the $1/x$ dependence predicted by both the theories of BPP and Torrey. The experimental values of T_1 are consistently higher than predicted, but this may be explained by the systematic error in the data and the effects of exchange.

The activation energies obtained from the temperature dependence of T_1, T_2, and the diffusion constant are in reasonable agreement. The activation energies for the mixtures are consistently lower than the value for pure He^3 at the same molar volume. The high-temperature intercept of D is within a factor of 4 of its pure He^3 value. The diffusion constant at the T_1 minimum is in better agreement with the Torrey theory than the BPP theory.

The T_1 data in the plateau region support the idea of a single spectral density for each solid phase. The concentration dependence of the spectral density only appears in ω_e (which is proportional to $\sqrt{x}$ and in the zero-field limit of T_1) [$T_1(0)$ is proportional to $1/\sqrt{x}$]. The plot of $[T_1(0)/T_1]$ as a function of $(\omega_0/\omega_e)^2$ thus gives a curve that is independent of concentration. The exchange interaction also appears to be independent of concentration, i.e., the overlap between two neighboring He^3 atoms depends only on the molar volume and not on the He^3 concentration.

The T_2 data in the plateau region is not in agreement with the theory obtained by allowing the moments of the line shape to become concentration-independent. This deviation from the theory is qualitatively explained by postulating the existence of two spin species: those that strongly experience the effects of exchange and those that do not. A small fraction of the isolated spins is then shown to dominate the relaxation process.

Note added in proof. Another possible explanation for both the concentration dependence of $J_1(\omega_0)$ and the small values of T_2 which are measured in the specimens formed with 1.94% He^3 is

that the He^3 atoms interchange rapidly with the He^4 atoms in a process similar to that of the He^3 exchange. The effects of such motion would essentially be similar to that of vacancies and T_2 would be expected vary as $T_2^{-1} \sim M_2(x)\tau_{34}$, where τ_{34} is the mean time between the interchange of He^3 atoms with He^4. For the specimen listed in Table V at 21.0 cm^3 with $x = 0.0194$, the measured value of T_2 is 10 msec and the value deduced for τ_{34} is $\sim 1 \times 10^{-5}$ sec. The details of this model are currently being investigated with more dilute specimens of He^3 in He^4.

ACKNOWLEDGMENTS

The authors would like to express their gratitude to Professor John W. Wilkins (Cornell) and Professor Robert A. Guyer (Duke) for many useful and stimulating conversations. They would also like to thank Professor David M. Lee (Cornell) for the use of research facilities and for helpful conversations about He^3-He^4 mixtures.

---

*Research supported in part by the National Science Foundation, through Contract No. GP-9343 and by the Advanced Research Projects Agency, through the Materials Science Center at Cornell University, MSC Report No. 1202.

†Present address: Sandia Corporation, Albuquerque, N. M.

[1]H. A. Reich, Phys. Rev. 129, 630 (1963).

[2]R. L. Garwin and A. Landesman, Phys. Rev. 133, A1503 (1964).

[3]M. G. Richards, J. Hatton, and R. P. Giffard, Phys. Rev. 139, A91 (1965).

[4]R. C. Richardson, E. Hunt, and H. Meyer, Phys. Rev. 138, A1326 (1965), and references contained therein.

[5]R. C. Richardson, A. Landesman E. Hunt, and H. Meyer, Phys. Rev. 146, 244 (1966).

[6]L. H. Nosanow and C. M. Varma, Phys. Rev. Letters 20, 912 (1968).

[7]R. A. Guyer and L. I. Zane, Phys. Rev. 188, 445 (1969).

[8]L. H. Nosanow and W. J. Mullin, Phys. Rev. Letters 14, 133 (1965).

[9]A. L. Thomson, H. Meyer, and P. N. Dheer, Phys. Rev. 132, 1455 (1963).

[10]R. P. Giffard and J. Hatton, Phys. Rev. Letters 18, 1106 (1967).

[11]H. D. Cohen, P. B. Pipes, K. L. Verosub, and W. M. Fairbank, Phys. Rev. Letters 21, 677 (1968).

[12]M. G. Richards and J. M. Homer, in *Proceedings of the Eleventh International Conference on Low Temperature Physics*, edited by J. F. Allen, D. M. Finlayson, and D. M. McCall (University of St. Andrews Printing Dept., St. Andrews, Scotland, 1969), Vol. 1, p. 340.

[13]M. Bernier and A. Landesman, Solid State Commun. 7, 529 (1969).

[14]W. N. Yu and H. A. Reich, Solid State Commun. 7. 1521 (1969).

[15]H. R. Glyde, Phys. Rev. 177, 272 (1969).

[16]S. R. Hartmann, Phys. Rev. 133, A17 (1964).

[17]E. R. Hunt, R. C. Richardson, J. R. Thomson, R. A. Guyer, and H. Meyer, Phys. Rev. 163, 181 (1967).

[18]N. Bloembergen, E. M. Purcell, and R. V. Pound, Phys. Rev. 73, 679 (1948).

[19]J. H. Van Vleck, Phys. Rev. 74, 1168 (1948).

[20]P. W. Anderson and P. R. Weiss, Rev. Mod. Phys. 25, 269 (1953).

[21]R. Kubo and K. Tomita, J. Phys. Soc. Japan 9, 888 (1954).

[22]A. Abragam, *The Principles of Nuclear Magnetism* (Oxford U. P., New York, 1961), p. 436.

[23]J. F. Jarvis, D. Ramm, and H. Meyer, Phys. Rev. 170, 320 (1968).

[24]E. L. Hahn, Phys. Rev. 80, 580 (1950).

[25]W. G. Clark, Rev. Sci. Instr. 35, 316 (1964).

[26]H. Y. Carr and E. M. Purcell, Phys. Rev. 94, 630 (1954).

[27]W. J. Mullin, Phys. Rev. Letters 20, 254 (1968).

[28]E. R. Grilly and R. L. Mills, Ann. Phys. (N. Y.) 8, 1 (1959).

[29]E. R. Grilly and R. L. Mills, Ann. Phys. (N. Y.) 18, 250 (1963).

[30]D. F. Holcomb and R. E. Norberg, Phys. Rev. 98, 1074 (1955).

[31]H. C. Torrey, Phys. Rev. 92, 962 (1953).

[32]E. H. C. Parker, H. R. Glyde, and B. L. Smith, Phys. Rev. 176, 1107 (1968).

[33]A. V. Chadwick and J. A. Morrison, Phys. Rev. Letters 21, 1803 (1968).

[34]W. M. Yen and R. E. Norberg, Phys. Rev. 131, 269 (1963).

[35]C. Kittel and E. Abrahams, Phys. Rev. 90, 238 (1953).

[36]G. Ia. Glebashev, Zh. Eksperim. i Teor Fiz. 30, 612 (1956) [Soviet Phys. JETP 3, 643 (1956)].

[37]H. Kumagai, K. Ono, I. Hayashi, H. Abe, J. Shimada, H. Shono, and H. Ibamoto, Phys. Rev. 83, 1077 (1951).